Anisotropic Dynamical Scaling near the Vortex-Glass Transition of Twinned $YBa_2Cu_3O_{7-\delta}$

J. Kötzler, M. Kaufmann, G. Nakielski, and R. Behr
Institut für Angewandte Physik, Jungiusstrasse 11, D-20355 Hamburg, Germany

W. Assmus
Physikalisches Institut, Universität Frankfurt am Main, Robert-Mayer-Strasse 4-6, D-60325 Frankfurt am Main, Germany
(Received 6 August 1993)

The complex electrical conductivity $\sigma(\omega)$ is determined from the linear ac susceptibility between 3 Hz and 3 MHz measured in fields between 0.4 and 12 T parallel and perpendicular to the c axis of a twinned crystal. Dynamical scaling of $|\sigma|$ and σ''/σ' reveals ordering temperatures $T_g(\mathbf{B})$ and field-independent scaling functions by using the variable $(T_{c2}-T_g)/|T-T_g|$. For $\mathbf{B} \perp \mathbf{c}$, the critical exponents ν and z agree with values obtained on films indicating isotropic vortex-glass fluctuations, whereas those for $\mathbf{B} \parallel \mathbf{c}$ indicate elongated fluctuations in the c direction mediated by correlated pinning via the edges of twin boundaries.

PACS numbers: 74.25.Nf, 74.60.Ge, 74.72.Bk

Based on early indications and suggestions for a glassy vortex state in a granular high-T_c superconductor [1], Fisher *et al.* [2,3] argued that in the absence of a driving current j this state represents a thermodynamic equilibrium phase emerging from a vortex liquid below some transition line $T_g(\mathbf{B})$. In clear distinction to the predictions of the flux creep [4] and thermally activated flux flow [5] models, which yield genuine superconductivity, i.e., zero resistance $\rho(j \to 0)$, only at zero temperature, the vortex glass (VG) is characterized by $\rho = 0$ for all temperatures below $T_g(\mathbf{B})$. Convincing evidence for the existence of this continuous phase transition has been provided by a number of scaling analyses of nonlinear voltage-current isotherms for $YBa_2Cu_3O_{7-\delta}$ (YBCO) [6–14]. The principal scaling variable of the VG transition is the glass correlation length $\ell \sim |T - T_g|^{-\nu}$ describing the diverging size of glassy islands and of lakes of vortex fluid above and below $T_g(\mathbf{B})$, respectively, and also the increasing lifetime of these fluctuations $\tau \sim \ell^z$.

The present physical interest in the VG transition is focused on the not yet well understood effect of the possible types of disorder. The original "isotropic" VG model of Fisher *et al.* [2,3] considered weak pinning to point defects which, due to charge doping, is intrinsic for all high-T_c materials. According to subsequent mean-field (MF) work by Dorsey *et al.* [15], (i) the VG transition may arise from a random spatial distribution of T_c and (ii) critical fluctuations lead to real exponents larger than the MF limits, $\nu_{MF} = 1/2$ and $z_{MF} = 4$. Fisher *et al.* [3] also indicated the possibility of anisotropic vortex fluctuations, characterized by a superdivergence of the correlation length parallel to $\mathbf{B}$, $\ell_z \sim \ell^{1/\zeta}$, with $0.5 \le \zeta < 1$. More recently, Nelson and Vinokur [16] considered the case of columnar pinning, either implemented artificially or originating from the mosaic of twin planes intrinsically present in bulk YBCO. Based on the Bose glass (BG) model and ignoring point defects they predicted a transition at T_{BG} to the vortex glass, characterized by $\zeta = 0.5$, for fields applied parallel to the disordered columns.

On the experimental side, the exponents obtained from scaling of the nonlinear resistivity $\rho(j)$ of YBCO *films* with $\mathbf{B} \parallel \mathbf{c}$ seem now to converge to the values $\nu = 1.7(1)$ and $z = 5.6(3)$ (see Table I), which signals the presence of one universality class of critical fluctuations. Such a class is characterized by the symmetry of the ordered phase and is independent of microscopic details of the system, like the microstructure and the thickness of the film as long as the dimensionality $d = 3$ is preserved [17]. Very recently, Wöltgens *et al.* [13] obtained from $\rho(j)$ scaling the same exponents for $\mathbf{B} \perp \mathbf{c}$ and interpreted this as an evidence against a BG phase. The exponents of films are close to those of the class of the $d = 3$ Ising spin glass [18], characterized by broken ergodicity, and are somewhat lower than values obtained from simulations

TABLE I. Critical exponents from $\rho(j)$ and $\sigma(\omega)$ scaling based on isotropic weak pinning [$\ell_z = \ell$ in Eq. (1)].

YBCO	T_c (K)	B	Exp.	ν	z	Ref.
Crystals	88.0	$\parallel$ c	$\rho(j)$	2.0(1.0)	3.4(1.5)	[6]
	92.9	$\parallel$ c	$\rho(j),\sigma(\omega)$	0.70(5)	3.0(2)	[7,23]
	88.1	$\parallel$ c	$\sigma(\omega)$	3.1(3)	3.1(3)	a
	88.1	$\perp$ c	$\sigma(\omega)$	1.6(3)	6.3(3)	a
Films	89	$\parallel$ c	$\rho(j)$	1.8	4.7	[8]
	90	$\parallel$ c	$\rho(j)$	1.8(2)	6(2)	[9]
	85.5	$\parallel$ c	$\rho(j)$	1.2(6)	5.6(1.0)	[10]
	87.5	$\parallel$ c	$\rho(j)$	1.8(1)	5.0(2)	[11]
	88	$\parallel$ c	$\rho(j)$	1.6(2)	5.5(5)	[12]
	87	$\parallel, \perp$ c	$\rho(j)$	1.7(1)	5.8(1)	[13]
	90	$\parallel$ c	$\sigma(\omega, T_c)$	···	5.6	[22]
	88.5	$\parallel$ c	$\sigma(\omega, T_c)$	···	3.7(5)	[24]
	91	$\parallel$ c	$\sigma(\omega)$	1.7(2)	5.5(5)	[29]
Ceramic	90		$\rho(j)$	1.1(2)	4.6(2)	[14]
Mean field	···	···	simul.	0.5	4	[15]
Gauge glass	···	···	simul.	1.3(4)	4.7(7)	[19]
Spin glass	···	···	simul.	1.3(3)	6.1(3)	[18]

[a]This work.

0031-9007/94/72(13)/2081(4)$06.00

of the gauge glass model [19]. However, the applicability of these models to the VG has been questioned by Blatter *et al.* [20]. The present work is devoted to the VG transition in *crystals*, where less conclusive information is available. For $\mathbf{B} \parallel \mathbf{c}$ of twinned crystals, Gammel *et al.* [6] found $\nu = 2(1)$ and $z = 3.4(1.5)$ and Yeh *et al.* [7] $\nu = 0.7$ and $z = 3.0$, which significantly differ from the "universal" values observed on films. It was proposed [17] to interpret these results in terms of the anisotropic BG model, which leads to exponents of the transverse VG correlations, $\nu = 1.0(5)$ and $z = 6.8(3.0)$, being closer to the "isotropic" values. In order to provide a stringent test of this hypothesis of linearly correlated pinning in bulk YBCO, we present here a comprehensive scaling analysis above and below $T_g(\mathbf{B})$ for the field parallel and perpendicular to the c axis of a twinned crystal.

Our main results are isotropic exponents for $\mathbf{B} \perp \mathbf{c}$ (see Table I), whereas for $\mathbf{B} \parallel \mathbf{c}$ we find $\nu = z = 3.1(3)$. This provides the first direct evidence for anisotropic dynamic scaling, which we ascribe to the edges of the twin planes located at the mosaic boundaries and running parallel to the c axis. This picture is consistent with recent neutron Bragg diffraction from the vortex lattice of YBCO [21]: For $\mathbf{B} \parallel \mathbf{c}$ fourfold short range order is found, which can be related to pinning by the mosaic of twins, while for large angles between $\mathbf{B}$ and $\mathbf{c}$ a sixfold symmetry distorted by the electronic anisotropy is observed. We also examined for the first time the effect of the vortex density on dynamic scaling functions for fields between 0.4 and 12 T. We find their shape to be unchanged, which we attribute to collective pinning [20], since the critical fluctuations *a priori* contain many vortices, $\ell \gg \sqrt{\phi_0/B}$. On the other hand, we observe a significant effect of $\mathbf{B}$ on the amplitude of the scaling variable, i.e., the VG correlation length which interestingly can be expressed in terms of the distance of the glass transition from T_{c2}. This feature and the shape of the scaling function deserve further theoretical attention.

We examine here the scaling behavior of the *linear* dynamic conductivity $\sigma(\omega)$, for the modulus and phase of which the following relations have been predicted [3,15]:

$$|\sigma(\omega)| = (\tau/\ell_z) S_{\pm}(\omega\tau), \tag{1a}$$

$$\arctan(\sigma''/\sigma') = P_{\sigma}(\pm\omega\tau), \tag{1b}$$

where $S_{\pm}$ and $P_{\sigma}(\pm x)$ are homogeneous functions above and below $T_g(\mathbf{B})$, respectively. Unlike the nonlinear resistance, the linear response function $\sigma(\omega)$ probes directly the (currentless) equilibrium state. Using the conventional technique, this quantity has been studied in a few cases [22–24]. As a contact-free method we employ here the complex linear ac susceptibility $\chi(\omega)$ measured by a carefully balanced and calibrated mutual inductance between 3 Hz and 3 MHz parallel to the static field $\mathbf{B}$. Typical results are shown in Fig. 1(a). The linearity of the response was checked by variation of the ac amplitude down to 0.1 μT, which generates a driving current density as low as $j_{rf} = 1$ A/cm^2 circulating around the sample cylinder ($R = 1.4$ mm) within $\lambda_s \gtrsim 1$ μm in the present range of temperature and fields [25]. The resulting Lorentz force $\mathbf{f}_L = \mathbf{j}_{rf} \times \boldsymbol{\phi}_0$ pushes the vortices towards the center of the sample, and their diffusion is monitored by $\chi(\omega)$. After correcting for finite sample size and numerically inverting the complex Bessel functions relating $\chi(\omega)$ and the penetration depth $\lambda(\omega)$, $\chi(\omega) = -1 + 2\lambda I_0'(R/\lambda)/RI_0(R/\lambda)$, we evaluate the dynamic conductivity from $\sigma(\omega) = (i\mu_0\omega\lambda^2)^{-1}$ [25,26]. The validity of this evaluation was confirmed well above T_g, where the classical skin effect was observed, $\mathrm{Re}\lambda^2 = 0$ and $\mathrm{Im}(\lambda^2) \sim \omega^{-1}$ [see Fig. 1(b)]. Referring to a recent systematic study by Claus *et al.* [27], our values for T_c= 88.1 K, ΔT_c(10%–90%) = 2 K, and $\rho_n(0) = 55$ $\mu\Omega$ cm reveal the present melt-grown crystal [28] as overdoped with $\delta = 0.05$. More technical details will be published elsewhere [29].

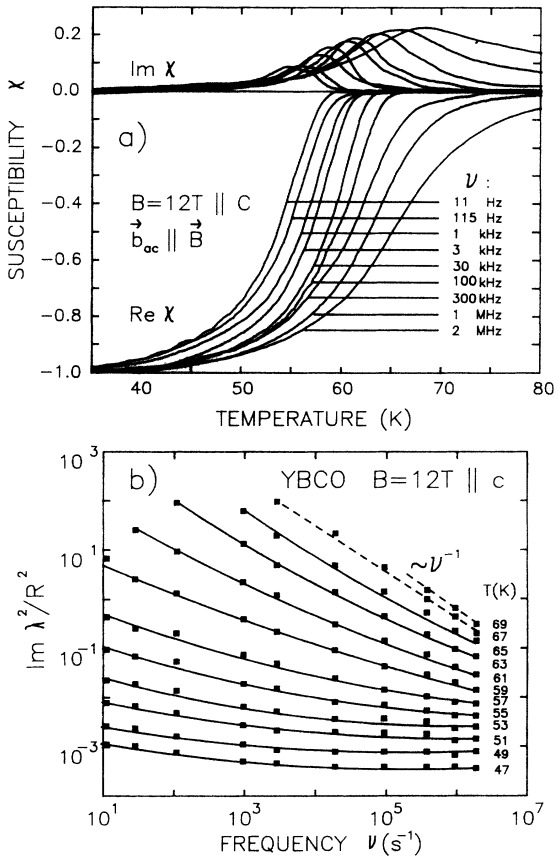

FIG. 1. (a) Dynamic susceptibility measured in $B = 12$ T applied parallel to the c axis. (b) Imaginary part of the squared magnetic penetration depth determined from $\chi(\nu)$; full curves obey scaling; dashed, normal skin effect.

The deviation of the frequency dependence of λ^2 from skin effect appearing below 69 K in Fig. 1(b) is accompanied by significant screening. In Fig. 2(a) this behavior is illustrated by the phase of $\sigma(\omega)$, $\sigma''/\sigma' = \mathrm{Re}\lambda^2/\mathrm{Im}\lambda^2$, plotted versus a scaled frequency. Obviously, within

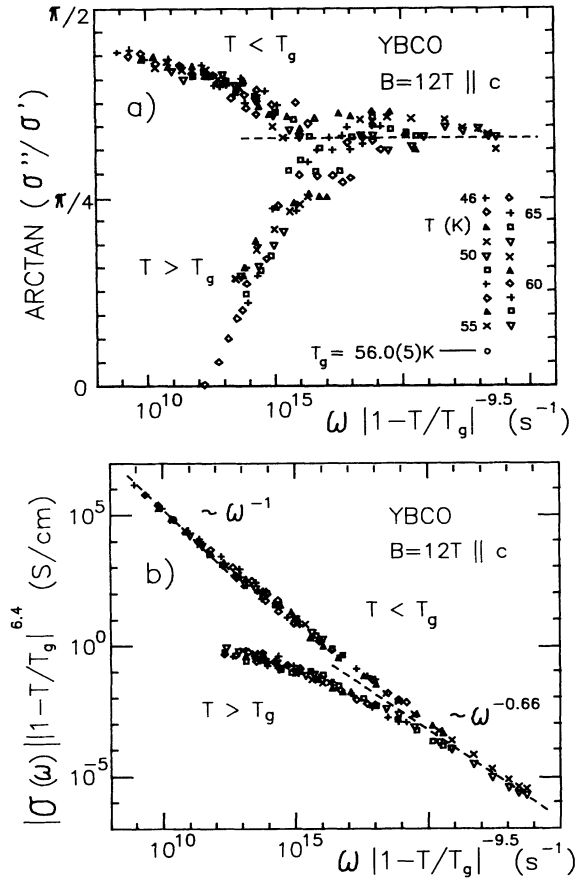

FIG. 2. Phase (a) and scaled amplitude (b) of the linear conductivity versus scaled frequency based on the data in Fig. 1. Dashed lines indicate the asymptotic behaviors predicted by the dynamic scaling [3,15].

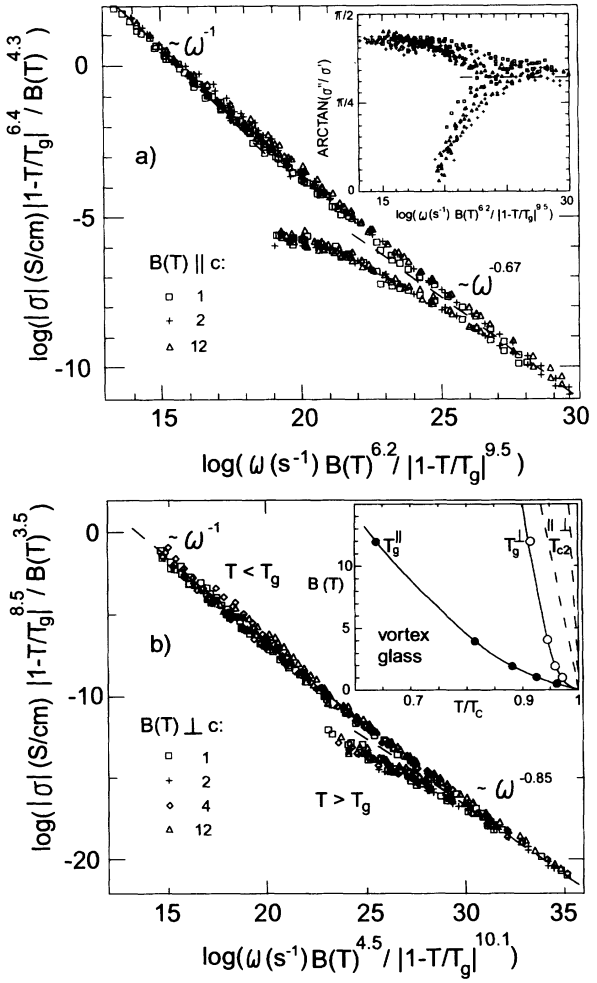

FIG. 3. Effects of the field **B** on the scaling variables for $|\sigma(\omega)|$ measured with **B** $\parallel$ **c** (a) and $\perp$ **c** (b). Full lines are calculated from Eq. (3). Inset shows the glass and transition lines $T_{c2}^{\parallel}$ and $T_{c2}^{\perp}$ from Ref. [30].

a small temperature interval, $\Delta T_g = \pm 0.5$ K, the frequency derivative of the isothermal phases changes sign. According to the scaling hypothesis, Eq. (1b), this is clear evidence for the thermodynamic phase transition at $T_g = 56.0$ K defined by $P_\sigma(\infty) = (\pi/2)(1 - 1/\zeta z)$, i.e., $dP_\sigma/d\omega = 0$. Using this T_g to scale the frequencies by $\tau^{-1} \sim \mid 1 - T/T_g \mid^{\nu z}$, one does indeed find the data to collapse on a single curve, $P_\sigma(\omega\tau)$, which characterizes a continuous phase transition. The accuracy for the exponent νz can be improved by scaling the amplitude of $\sigma(\omega)$ by $\sigma_+(0) \sim \mid 1 - T/T_g \mid^{-s}$ shown in Fig. 2(b). The results are rather impressive, because all the essential features predicted by the scaling theory of the VG transition [3,15], like $S_+(x \to 0) = \text{const}$, $S_-(x \to 0) \sim x^{-1}$, and $S_\pm(x \to \infty) \sim \omega^{(1/\zeta z)-1}$ are reproduced. Also the width of the critical region, which is largest for this highest applied field of 12 T, $|\Delta T| / T_g \approx 0.2$, and decreases to 0.03 at 0.4 T, is not inconsistent with the theoretical estimate [3].

Using the exponents $\nu z = 9.5$ and $s = \nu(z - 1/\zeta) = 6.4$ obtained at 12 T, we were able to scale also the dynamic conductivities measured at all lower fields. Since the shapes of the resulting scaling functions looked very similar, we compared them directly to each other by allowing the scaling variables to vary with field. Figure 3(a) demonstrates that high powers of the field in the scaling variables do lead to a collapse on single curves for $P_\sigma(x)$ and $S_\pm(x)$. Figure 3(b) shows that this type of field scaling is also valid for **B** $\perp$ **c**, where the dynamic scaling performed at fixed fields around $T_g^{\perp} > T_g^{\parallel}$ yielded, however, different exponents, $\nu z = 10.1$ and $s = 8.5$, to be discussed below. First, we point out an interesting consequence of the B scaling. It can be completely ascribed to the field dependence of the (transverse) VG correlation length:

$$\ell(T, B) \sim \left(\frac{B^\beta}{|1 - T/T_g(B)|} \right)^\nu , \qquad (2)$$

with $\beta = 0.66(2)$ and $0.43(4)$ for **B** $\parallel$ **c** and **B** $\perp$ **c**, respectively. This novel result can be empirically inter-

preted by noting that the exponents β perfectly explain the transition lines for both field orientations, shown by the inset of Fig. 3(b),

$$1 - T_g/T_{c2} = (B/B_\Delta)^\beta. \quad (3)$$

This finding implies $\ell(T,B) \sim [(T_{c2} - T_g)/\,|\,T - T_g\,|]^\nu$, and hence the amplitude of ℓ to increase with the distance between T_g and T_{c2}, i.e., with growing superconducting order parameter $|\psi|^2$.

As the central result of the scaling analyses we discuss the exponents νz and s describing the criticality of τ and $\sigma(0)$. Let us start by adopting the isotropic VG model, $\ell_z = \ell$, i.e., $\zeta = 1$, in order then to compare the results for ν and z to published data derived from the same model; see Table I. This comparison reveals two key features: (i) For $\mathbf{B} \parallel \mathbf{c}$, our exponent $z = 3.1(3)$ agrees with previous results on crystals, while (ii) for $\mathbf{B} \perp \mathbf{c}$ our values for z and ν agree with the average exponents of films, which include our results obtained on a twin-free film [29] using the present $\chi(\omega)$ method. Feature (ii) suggests attributing the critical vortex dynamics of films and of crystals with $\mathbf{B} \perp \mathbf{c}$ to *one* universality class of *critical* behavior, the exponents of which are much larger than those predicted by the MF approach [15]. Since ν and z are much closer to results from simulations of the isotropic gauge and spin glass models, we argue that they are indicative of *isotropic* fluctuations. Feature (i), on the other hand, reveals a value for z smaller than the MF result, which suggests relating the critical vortex dynamics in crystals with $\mathbf{B} \parallel \mathbf{c}$ to anisotropic scaling characterized by $\zeta < 1$. Because our scaling defines only two exponents, ζ cannot be determined. However, taking the lower limit $\zeta = 0.5$ [3] the resulting exponents $\nu' = \nu\zeta = 1.6(2)$ and $z' = z/\zeta = 6.1(2)$, which characterize the transverse correlations, assume the isotropic values. This indicates uncorrelated pinning perpendicular to the c axis, in contrast to correlated pinning parallel to $\mathbf{c}$. In view of the above mentioned Bragg patterns [21] and following Nelson and Vinokur [16], we tentatively associate this with the mosaic ($25 \times 25\ \mu m^2$) of twin plane ($d = 0.15\ \mu m$) colonies of our crystal. It is perhaps interesting to note that $\zeta = 1/2$ has been predicted [16] for the Bose glass, on the other hand, the estimates of the field effect on the transition line, $\beta = 1/4$, and of the field dependence of the length scale, e.g., $\ell \sim B^{-1/2}$ [16], are inconsistent with our results Eqs. (2) and (3). Finally, we attribute the isotropic scaling for $\mathbf{B} \perp \mathbf{c}$ to the absence of any anisotropy in between the CuO_2 layers: Because of their strong planar pinning [31] the vortices diffuse within these gaps via the excitation of circular loops by j_{rf} directed across the planes.

To conclude, through dynamical scaling of $\sigma(\omega)$ we have obtained clear evidence for thermodynamic transition lines $T_g(\mathbf{B})$ to a true superconducting vortex state in a twinned YBCO crystal with $\mathbf{c} \parallel \mathbf{B}$ and $\perp \mathbf{B}$. The values of the critical exponents indicate anisotropic vortex glass fluctuations for $\mathbf{B} \parallel \mathbf{c}$, which most likely arise from correlated pinning by lines of twin edges. Though the anisotropy exponent $\zeta = 0.5$ agrees with that of the Bose glass model, the distinct field effect on $T_g(\mathbf{B})$ and on the VG scaling parameters are at variance with the predictions based on this model. For $\mathbf{B} \perp \mathbf{c}$ isotropic scaling dominates $\sigma(\omega)$.

The authors thank E.H. Brandt (Stuttgart), K.H. Fischer (Jülich), Hartwig Schmidt (Hamburg), K. Scharnberg (Hamburg), and Harry Suhl (La Jolla) for useful discussions.

[1] K.A. Müller *et al.*, Phys. Rev. Lett. **58**, 1143 (1987).
[2] M.P.A. Fisher, Phys. Rev. Lett. **62**, 1415 (1989).
[3] D.S. Fisher *et al.*, Phys. Rev. B **43**, 130 (1991).
[4] P.W. Anderson and Y.B. Kim, Rev. Mod. Phys. **36**, 39 (1964).
[5] P.H. Kes *et al.*, Supercond. Sci. Technol. **1**, 242 (1989).
[6] P.L. Gammel *et al.*, Phys. Rev. Lett. **66**, 953 (1991).
[7] N.C. Yeh *et al.*, Phys. Rev. B **47**, 6146 (1993).
[8] R.H. Koch *et al.*, Phys. Rev. Lett. **63**, 1511 (1989).
[9] C. Dekker *et al.*, Phys. Rev. Lett. **68**, 3347 (1992).
[10] Y. Ando *et al.*, Phys. Rev. Lett. **69**, 2851 (1992).
[11] J. Deak *et al.*, Phys. Rev. B **48**, 1337 (1993).
[12] D.G. Xenikos *et al.*, Phys. Rev. B **48**, 7742 (1993).
[13] P.J.M. Wöltgens *et al.*, Phys. Rev. B **48**, 16826 (1993).
[14] T.K. Worthington *et al.*, Phys. Rev. B **43**, 10538 (1991).
[15] A.T. Dorsey *et al.*, Phys. Rev. B **45**, 523 (1992).
[16] D.R. Nelson and V.M. Vinokur, Phys. Rev. Lett. **68**, 2398 (1992); Phys. Rev. B **48**, 13060 (1993).
[17] C. Dekker *et al.*, Phys. Rev. Lett. **69**, 2717 (1992).
[18] A.T. Ogielski, Phys. Rev. B **32**, 5384 (1985).
[19] J.D. Reger *et al.*, Phys. Rev. **44**, 7147 (1991).
[20] See, e.g., G. Blatter *et al.*, Rev. Mod. Phys. (to be published).
[21] M. Yethiray *et al.*, Phys. Rev. Lett. **70**, 857 (1993); **71**, 3091 (1993).
[22] H.K. Olsson *et al.*, Phys. Rev. Lett. **66**, 2661 (1991).
[23] D.S. Reed *et al.*, Phys. Rev. B **47**, 6150 (1992).
[24] Hiu Wu *et al.*, Phys. Rev. Lett. **71**, 2642 (1993).
[25] M.W. Coffey and J.R. Clem, Phys. Rev. Lett. **67**, 386 (1991).
[26] E.H. Brandt, Phys. Rev. Lett. **67**, 2219 (1991).
[27] H. Claus *et al.*, Physica (Amsterdam) **200C**, 271 (1992).
[28] J. Kowalewski and W. Assmus, Eur. J. Solid State Inorg. Chem. **27** (1-2), 135–140 (1990).
[29] G. Nakielski *et al.* (to be published).
[30] U. Welp *et al.*, Phys. Rev. Lett. **62**, 1908 (1989).
[31] M. Tachiki and S. Takahashi, Solid State Commun. **70**, 291 (1989).